CHAPTER IV
EFFECT OF ORGANOCLAY DISPERSION ON MORPHOLOGY, CRYSTALLIZATION, THERMAL AND MECHANICAL PROPERTIES OF POLYPROPYLENE/LAYERED SILICATE NANOCOMPOSITES

4.1 Abstract

Polypropylene (PP)/layered silicate nanocomposites of varying three different organoclays modified by alkyl ammonium surfactants: CTAB; BTC; and DOEM, were prepared by melt intercalation technique in a co-rotating twin screw extruder. The polypropylene-graft-maleic anhydride (PP-g-MA) was used as a compatibilizer and the amount of each organoclay was varied from 1 to 7 wt%. The effect of alkyl ammonium surfactant structures and amount of organoclay were investigated. From the XRD result, the nanocomposites prepared from CTAB and BTC showed the intercalated morphology, while the nanocomposite prepared from DOEM showed the partially exfoliated morphology. All nanocomposites showed an improvement in both thermal and mechanical properties as compared to the pure PP and PP/PP-g-MA system and increased with increasing organoclay loading. Among three types of alkyl ammonium surfactants, the nanocomposite prepared from DOEM, having two tails and the longest alkyl chain length (2C18), gave the best morphological and physical property due to the better clay dispersion.

(**Key-words**: alkyl ammonium surfactant, organoclay; melt intercalation; polypropylene; nanocomposite)

4.2 Introduction

Polymer/layered silicate nanocomposites have been recognized as one of the most promising materials because of their superior physical and mechanical properties compared to those of their conventional filled composites or micro-composites (Okada, 1990; Manias, 2001; Lee, 2002). Some properties that are dramatically improved include physical and mechanical properties, thermal and flame-retardant characteristic (Modesti, 2006; Gilman, 1999; Bertini, 2006; Krishnamoori, 1996), and barrier performance properties (Manias, 2001; Lee, 2005; Krump, 2006). All improvements generally obtain at very low filler loadings of less than 5 wt%.

Polypropylene (PP) is one of the most widely used thermoplastic polymers for preparing polymer/layered silicate nanocomposites due mainly to its low price and balanced properties. The great advantages of producing clay filled-PP composites is, however, often cited for its great processability and low cost to replace existing engineering and functional materials. It is attractive as automotive and packaging materials. The present efforts to investigate PP based nanocomposites are focused on uniformity dispersing modified clay particles in nonpolar matrices to maximize their physical and mechanical properties. However, exfoliating nanoclay in PP has been challenging, as a result of difference in surface polarity between the clay and the pure polymer. Polypropylene, due to its hydrophobic nature, is not able to establish interface interactions as effective as to disperse the nanoparticles by intercalation and to stabilize the morphology; suitable surfactants as an inorganic surface modifiers and a functionalized polyolefins as matrix or as compaibilizer are generally used: combined hydrophobic and hydrophilic interactions grant both the effects, even if concentration/amount of polar groups is very low (generally les than 1% by mol) (Passaglia, 2005; and Ciardelli, 2008). In this way, the preparation of PP nanocomposites with well-established dispersion level reflecting in good performances, particularly for gas barrier properties, is possible and generally the thermal analysis of samples highlighted that the cooperative relaxation of polyolefin chains in the composite becomes weak due to the restricted mobility of the chains in the present of clay platelets (Hambir *et al.* 1937).

Among the existing clays layered silicates, i.e. montmorillonite (MMT), are considered as the most effective nanofillers for the preparation of polymer nanocomposites. Silicate clays dominate as low cost, ready availability and nonisometric structure derived from high aspect ratio and, thus possessing high surface area for polymer-filler interactions. Since the layered silicate surface is hydrophilic and incompatible with most polymers, especially polyolefins. In order to render the hydrophilic clay more organophilic, ion-exchange modification with cationic surfactant bearing long alkyl chains is generally performed. These voluminous organic ions increase the interlayer distance, lower the surface energy by improving the wetting characteristic of the layers and make possible intercalation with polar polymers (Giannelis, 1996).

It is worthy that the chemical structure of the organic surfactants used to modify the layered silicate surface plays very important role to the morphology of the nanocomposites. Several works have shown that alkylammonium salts allowed to increasing the interlayer spacing and improved the interactions between the clay and the polymer matrix. Lee and Kim (2002) and Hackett *et al*. (1998) investigated the effect of alkyl chain length the cationic surfactants to the interlayer spacing of the organoclays. Yang *et al*. (1999) reported an importance of the surfactant on the properties of polyimide/organoclay systems obtained by in situ polymerization. Fornes *et al*. (2002) reported the study of nylon 6/organoclay with different types of surfactants. Various aspects such as the level of saturation, the alky chain length, the number of alkyl chains and the size of cationic group has been investigated. The selection of a suitable organoclay is equally critical for producing polymer nanocopomposites with excellent exfoliation. Structural aspects of the surfactant like the number and length of alkyl tails, degree of saturation, etc. along with the amount of surfactant loading on the clay may significantly affect the exfoliation degree (Fornes, 2002; Yoon, 2003; Stretz, 2004). Fornes *et al*. (2002 and 2004) found that organic modifier one long alkyl tail led to higher level of organoclay exfoliation in nylon 6 than those having two alkyl tails. This is believed to be the result of higher affinity that nylon 6 has for the pristine surface of the organoclay than for the largely aliphatic organic modifiers. On the other hand, nanocomposites made from a non-polar polymer like LLDPE showed completely opposite trends (Hotta and Paul,

2004), i.e. the two-tailed organoclay formed nanocomposites with better exfoliation state and mechanical properties than the one-tailed organoclay.

More recent theoretical approach, reasonably explaining some important features and results (particularly about the mechanical and rheological behavior of PP/clay nanocomposites), evidenced that at increased amount of organoclay (up to 2 wt%) a three-dimensional filler network is formed and it plays an essential role on the dynamics behaviour of macromolecular PP chains: the physical jamming and connecting of nanoscale dispersed fillers (randomly oriented clay tactoids with locally located layers) generates a structure larger than that of intercalated and exfoliated structures that can be regarded that as mesoscopic structure where motion of PP chains is restricted (Wang *et al.* 2006). This completely interconnected structure (the percolated clay network), where also the silicate sheets are incapable of freely rotating, is generally different and depends on starting amount of inorganic fillers (for organoclay content above the threshold) and, more important, is reported to severely affect the macroscopic properties of PP/clay nanocomposites: before the formation of percolated clay network, the effect of inorganic platelets on the restricted motion of PP chains can be neglected.

Based on above considerations, the main objective of this present contribution is to study the effect of alkyl chain length and other aspects of the surfactant structures on the morphology and physical properties. PP/organoclay nanocompsites were prepared by melt intercalation. The structure-property relationship, thermal stability, and mechanical of intercalated nanocomposites have been discussed as a function of both the organoclay loading and types of alkyl ammonium surfactant. Specific comparison among commercial surfactants was made by addressing structural variations. Wide angle X-ray spectroscopy (WAXS) and Transmission electron microscopy (TEM) were used to study the nanocomposite morphology. Thermal stability, Crystallization behavior and mechanical properties were also studied.

4.3 Results and Discussion

4.3.1 Purification of Na-bentonite

Figure 4.1 shows the XRD patterns of Na-bentonite, purified bentonite, and Na-montmorillonite. The X-ray diffractogram of the Na-bentonite shows the peak of montmorillonite as a major component with (001) reflection peak at $2\theta = 5.7°$ that corresponds to the interlayer spacing $(d_{001}) = 1.55$ nm. Beside the montmorillonite, quartz (Q) and feldspar (F) were present as accessory impurities (Ramos et $al.$ 2005). The amount of quartz that compared to the main peak d_{001} is approximately 35%. After purification, the feldspar was clearly removed; however the quartz was not, remaining in a small amount (3 % as compared to the d_{001} peak) presented at the peak position $2\theta = 21.92°$. The X-ray diffractogram of the purified bentonite gave the interlayer spacing $(d_{001}) = 1.52$ nm $(2\theta = 5.82°)$.
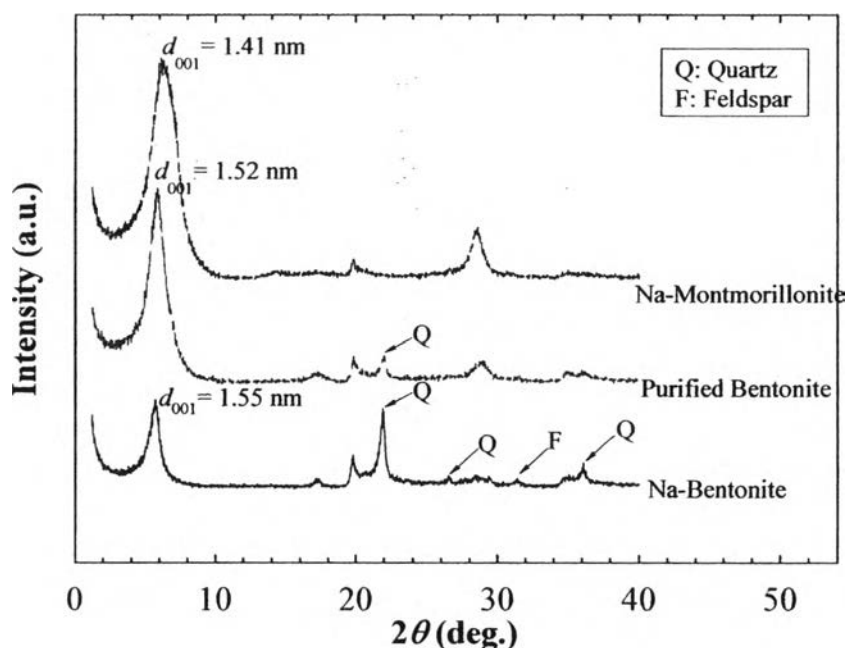
Figure 4.1 XRD patterns of Na-bentonite, Purified bentonite and Na-montmorillonite.

The swelling power, cation exchange capacity (CEC), and the EDX results of the Na-bentonite (local clay) and purified bentonite were compared with Na-montmorillonite, as shown in Table 4.1. The swelling power was measured by the following method: 2 g of clays were poured into 100 ml of distilled water (or n-dodecane) in a mass cylinder. After 24 h, the apparent volumes of the swelling clays were measured (Lee $et\ al.$ 2004), and the CEC value was measured by the methylene blue index (Rytwo $et\ al.$ 1991). The swelling and CEC value are important factors to determine the grade of the clay minerals. The local bentonite has swelling and CEC equal to 22 ml/2g and 50 meq/100g, respectively. After purification, the swelling and CEC were increased to 35-40 ml/2g and 90 meq/100g respectively. These results were similar to the commercial Na-montmorillonite. The improvement in swelling and CEC of the purified bentonite was caused by the lower interaction between cations, especially Ca^{2+}, in the galleries and the silica tetrahedral. If in the galleries have high percentage of Ca^{2+} cation, the swelling and CEC should be lower than that of the Na^+ cation due to the strong interaction between Ca^{2+} and silica tetrahedral (Lee $et\ al.$ 2004) This phenomenon corresponded to the elemental analysis by EDS; the quantitative analysis of the local bentonite gave %Ca = 1.26% and %Na = 3.04%. For the purified bentonite, the Ca element was not observed. Conversely, the percentage of Na was increased (3.75%) resulting to the higher swelling and CEC value. These results suggest that besides the removal of quartz and feldspar as impurities, the dense Ca (in the form of $CaCO_3$) was also eliminated by the purification method.

Table 4.1 Swelling power, Cation Exchange Capacity and elemental analysis of Na-Bentonite, Purified Bentonite and Na-Montmorillonite

Clays	Swelling power (ml/2g)	CEC (meq/100g)	Elemental analysis (EDX)
Na-Bentonite	22	50	O, Na (4.03%)[a], Mg, Al, Si
Purified Bentonite	35-40	90	O, Na (3.04%)[a], Mg, Al, Si, K, Ca (1.26 %)[a]
Na-Montmorillonite	45	115	O, Na (3.75%)[a], Mg, Al, Si

[a]Quantitative analysis by Energy Dispersive X-ray spectrometer (EDS), OXFORD (link ISIS series 300).

4.3.2 Characterization of the Organoclay

It is well known that the structural aspects of the surfactants like the number and length of alkyl tail, degree of saturation, along with the amount of surfactant loading on the clay may significantly affect the degree of clay dispersion. In general, the longer surfactant chain length, the further apart the clay layers will be forced. This contributes to the increasing the volume occupied by the intragallery surfactants (LeBaron *et al.* 1999). Figure 4.2 shows the XRD patterns of the organoclays modified by various quaternary ammonium ions; CTAB-clay (one alkyl tail), BTC-clay (one alkyl tail and one benzyl group), and DOEM-clay (two alkyl tails) as shown in Table 4.2). It is clear that all organoclays show a shift of reflection peak to lower angles as compared to the pristine clay, corresponding to an increasing of d-spacing of 2.1, 2.3, and 6.5 nm for CTAB-clay, BTC-clay, and DOEM-clay, respectively. This evidence confirms that the molecules of ammonium ions were incorporated between the silicate layers. As expected, the d-spacing of the organoclay in crease with increasing the surfactant chain length. The increase in interlayer distance not only depends on the structure of surfactants but also the way that the surfactant molecules organize themselves between the silicate layers. For the case of CTAB-clay and BTC-clay, the surfactant molecules may organize in pseudo-trimolecular structure (Bonczeck, 2002 and Xi, 2004). A larger interlayer separation

of BTC-clay compared to that of CTAB-clay might be due to the benzyl bulky group. However, the increasing in d-spacing of DOEM-clay to 6.5 nm, suggest the paraffin-type bilayer arrangement of this surfactant (Bonczeck, 2002; Xi, 2004; Ray, 2003).
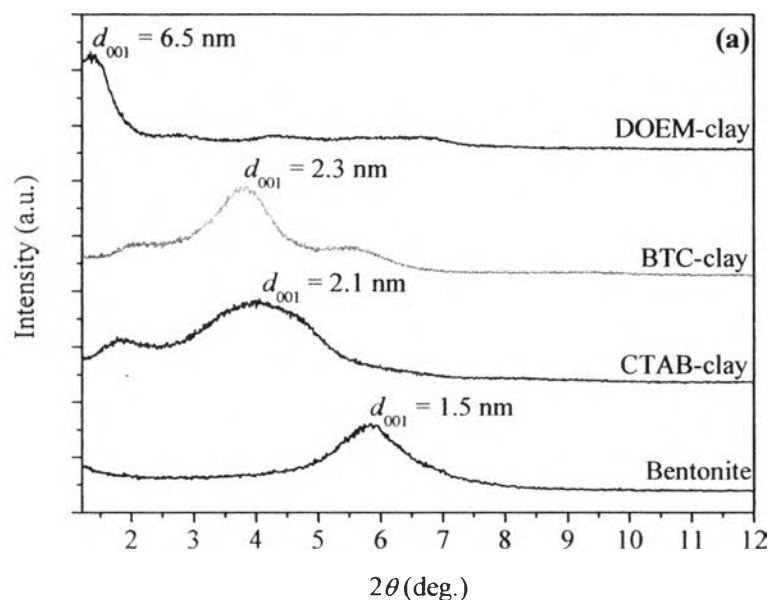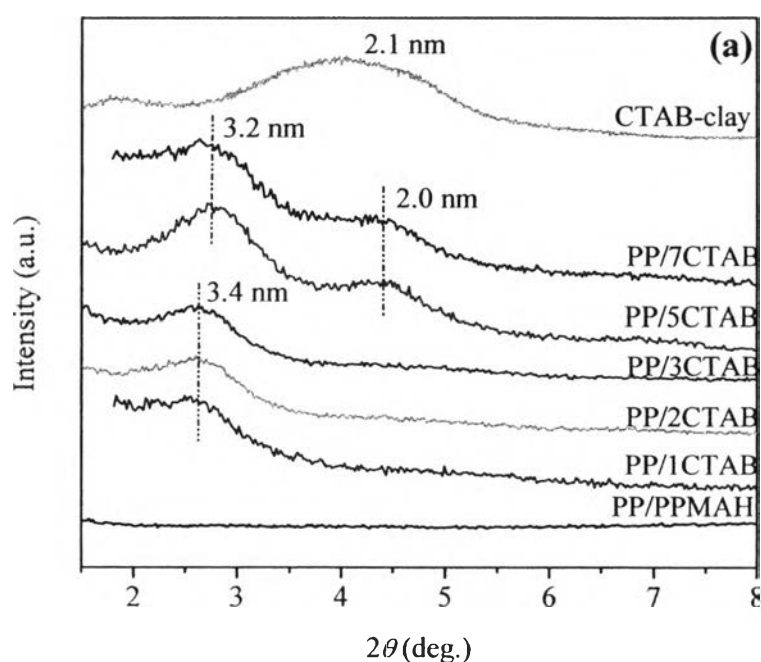

Figure 4.2 XRD patterns of the organoclays modified with different alkyl ammonium surfactants.
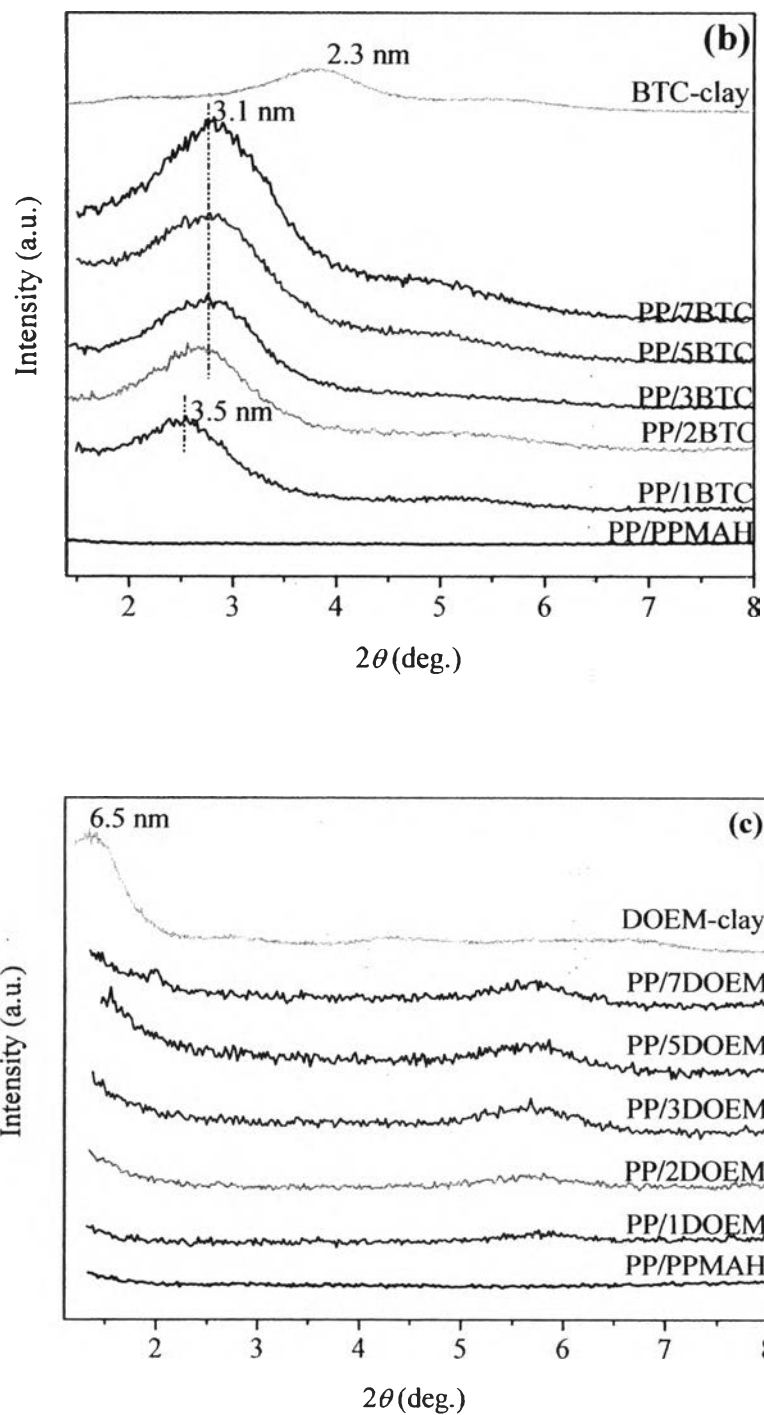
4.3.3 Structure of PP/Organoclay Nanocomposites

Figure 4.3 shows the XRD patterns of all PP/organoclay nanocomposites with various organoclays loading. The XRD patterns for the nanocomposite based on one alkyl tail in the structure (CTAB-clay) shown in Figure 4.3 (a), two groups of structure are evident: (a) the nanocomposite containing 1,2, and 3 wt% organoclay loading shows one reflection peak at $2\theta = 2.6°$ related to d-spacing of 3.4 nm, which indicates the intercalated structure; (b) the nanocomposites containing 5 and 7 wt% organoclay loading, two distinct reflection peaks are appeared; the first peak at $2\theta = 2.8°$ consistent with d-spacing of 3.2 nm and the second broad peak at the same angle of the CTAB-clay, suggests the presence of clay tactoids. The XRD patterns for the nanocomposites based on one
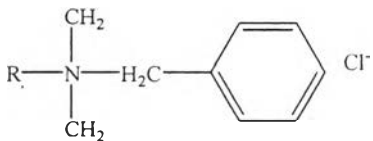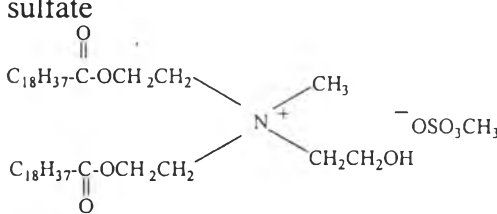
alkyl tail and one benzyl group in the structure (BTC-clay) as shown in Figure 4.3 (b), all samples show similar shift of reflection peak toward lower angels. The nanocomposite containing 1wt% organoclay shows peak at $2\theta = 2.5°$ related to d-spacing of 3.2 nm. For the others (containing 2, 3, 5 and 7wt% organoclay loading), reveal the same peak at $2\theta = 2.8°$ corresponded with d-spacing of 3.1 nm. This implies the formation of the intercalated structure. Interestingly, the XRD pattern for the nanocomposite based on the two alkyl tails in the structure (DOEM-clay) as shown in Figure 4.3(c) is suggestive of the exfoliated or partially exfoliated morphology, since the reflection peak at lower angles disappears. Moreover, it should be noted that the exfoliation degree in PP/organoclay system is independent on the organoclay content (Wang *et al.* 2005), which results in the dominant intercalated structure even if the clay content is low (1 wt%), particularly for CTAB and BTC-clay based nanocomposites. Increasing organoclay content seems to enhance the density of clay tactoids and layers in the PP matrix, resulting in a decrease of the ratio of the averaged spacing between neighboring particles to the average length of tactoids and layers. This will lead to gradual formation of spatially linked structure of dispered clay tactoids and individual layers in PP matrix, and ultimately to a "percolating filler network structure" as the clay content reaches a certain threshold (Wang, 2006 and Muksing, 2007).
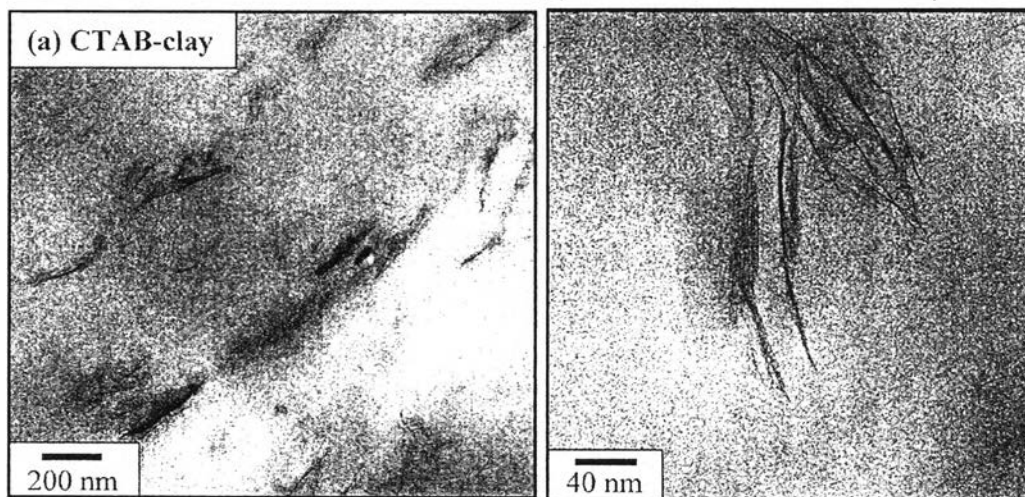
Figure 4.3 XRD patterns of PP nanocomposite based: (a) CTAB-clay, (b) BTC-clay, and (c) DOEM-clay, for various organoclay contents.

Table 4.2 Chemical structure of modifying agents and their interlayer spacing after organic modification

Organoclay	Chemical and Structure	d-spacing (d001)/ arrangement in the interlayer
CTAB-clay (one alkyl tail, C16)	Hexadecyltrimethylammonium bromide salt, $C_{16}H_{33}N^+(CH_3)_3$	2.1 nm pseudotrimolecular
BTC-clay (one alkyl tail (C14-C16) and one benzyl group)	N-alkyl dimethyl ammonium chloride R = 50%C_{14}, 40%C_{12},10%C_{16}	2.3 nm pseudotrimolecular
DOEM-clay (two alkyl tail, 2C18)	Methyl di-[(partially hydrogenated) tallow carboxyethyl]-2 dihydroxyethyl ammonium methyl sulfate	6.5 nm paraffin arrangement

[a]The basal spacing corresponds to the reflection peak (001) obtained from WAXS scan of the organoclays.

The selected TEM micrographs at low and high magnifications of 5wt% organoclay loading for each composite as shown in Figure 4.4 provide visible evidence of the conclusion from the XRD data. The nanocomposite based CTAB-clay (one alkyl tails) contains predominantly of an intercalated and small aggregarted silicate layers with tactoids (ordered stacks) thickness of 30 to 60 nm, length of less than 200 nm distributed throughout the polypropylene matrix as shown in Figure 4.4(a). Moreover, individual silicate layers are also evident with the thickness of several nanometers and length of about 100 nm. Therefore a broaden dispersion of aspect ratio of layered silicate particles is around 40 to 100. Similarly, the nanocomposite based BTC-clay (one alkyl tail and one benzyl group), is comprised of a large fraction of intercalated clay particles in addition to individually dispersed layers (see Figure 4.4(b)). For the nanocomposite based DOEM-clay (two alkyl tails) shown in Figure 4.4(c), reveal areas containing rather well exfoliated silicate layersand some clay tactoids with thickness of several nanometers and length of less than 100 nm. So, the aspect ratio of DOEM-clay particles is about 40 nm which is less than the other based nanocmposite samples.
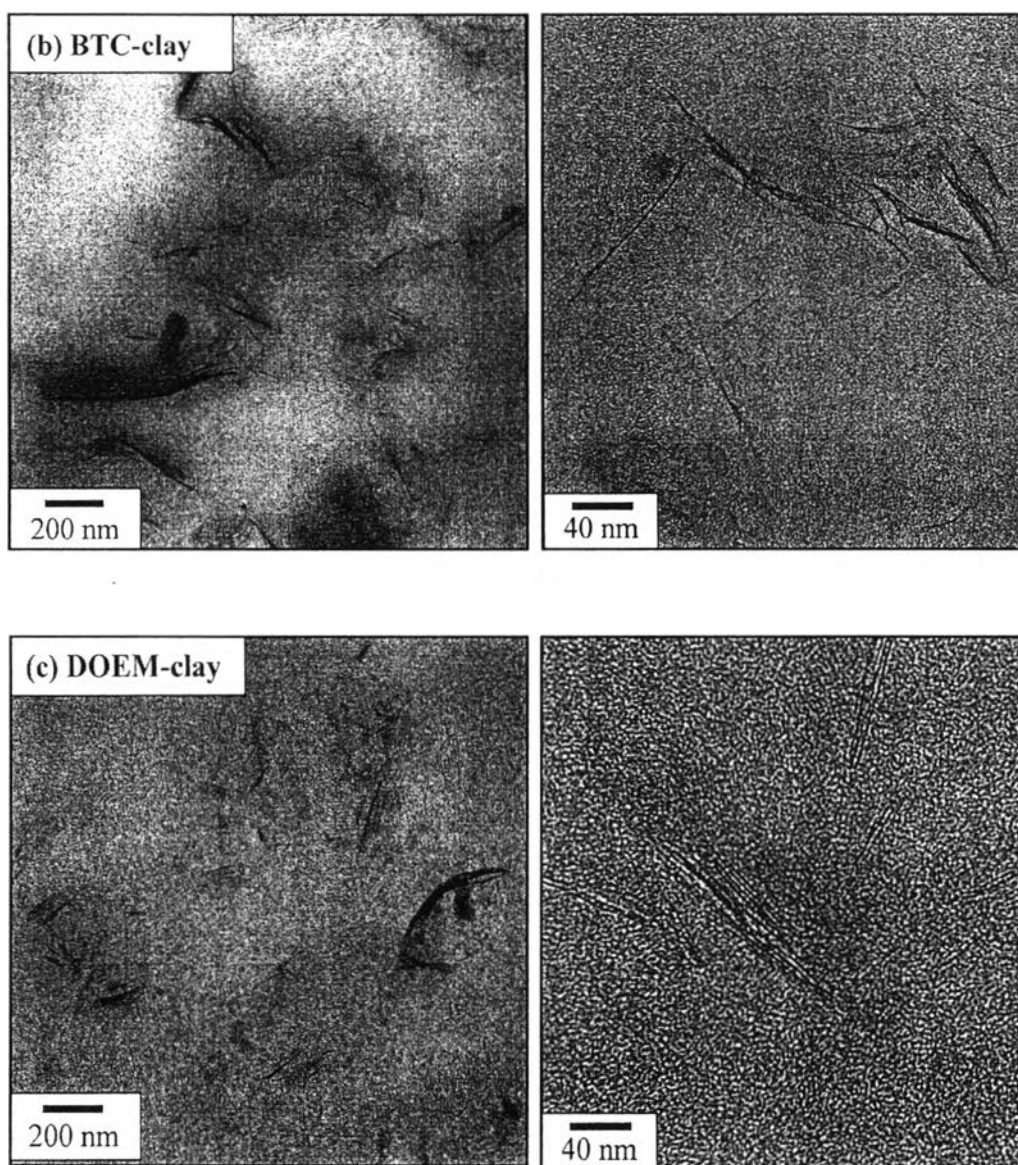
Figure 4.4 Representative TEM micrographs of PP nanocomposite based: (a) CTAB-clay, (b) BTC-clay, and (c) DOEM-clay, for 5wt% organoclay loading.

4.3.4 Thermal stability of PP/Organoclay nanocomposites

Thermal stability of PP/organoclay nanocomposites was analyzed by TGA as shown in Figure 4.5(a)-(c). The temperature corresponding to 10% and 50% of weight loss ($T_{10\%}$ and $T_{50\%}$) are summarized in Table 4.3. It is clear that all nanocomposites evidence a remarkable improvement at both lower and higher temperature as compared with the pure matrix. Indeed, the temperature corresponding to 10% of weight loss ($T_{10\%}$) for most nanocomposites is shifted to higher temperatures with increasing organoclay contents. This is similar to the results obtained by Bertini *et al.* (2006) and Tang *et al.* (2003), which is due to the intimate contact between the polymer molecules and the atom of inorganic crystalline layers is more extensive than that in a microcomposite, and at the same time there is a catalytic role by the layered silicates deriving from the Hoffman reaction of long chain surfactant which may accelerate the charring process at the beginning of polymer decomposition (Zanetti, 2002 and Tang, 2003). The degradation temperature at 50% of weight loss ($T_{50\%}$) for most nanocomposites is significantly shifted to higher temperature. This is may be attributed to the diffusion effect, which limits the emission of gaseous degradation products (Krump, 2006 and Duquense, 2003) and the ablative reassembling of the silicate layers which build up on the surface that insulates the underlying material and shows the escape of volatile product generated during decomposition (Tang *et al.* 2003).

Among three types of organoclay bases nanocomposites, CTAB-clay nanocomposite reveals the highest thermal stability. In this case there seems to be a combination of the amount of added clay and the morphology of the nanocomposites. At a relatively low amount of organoclay, the thermal stability increased with increasing organoclay content. In fact, the nanocomposite with 3 wt% CTAB-clay showed the best thermal stability, similar to that of the composite containing 7 wt% organoclay. However, further increase organoclay i.e. 5 wt% CTAB-clay, the thermal stability decreased. This may be due to the present of non-intercalated organoclay tactoids, which were less effective in blocking the heat transfer than the well dispersed single layers or intercalated tactoids in good agreement with XRD and TEM results. For PP/DOEM-clay based nanocomposites, on the other hand, 5 wt% organoclay exhibits the highest value of $T_{50\%}$ as confirmed by TEM image showing

organoclay exhibits the highest value of $T_{50\%}$ as confirmed by TEM image showing the good dispersion of the clay layers in polymer matrix. Unfortunately, for PP /BTC-clay based nanocomposites, showed the lowest thermal stability and there seemed no significant effect on $T_{50\%}$ with respect to the organoclay content. This might due to the presence of bulky benzyl group may inhibit the dispersion of the layered silicate in polymer matrix as reported by XRD result. It is noted that about 3 wt% organoclay loading in the nanocomposite may be a threshold before the formulation of a percolating filler network structure (Wang *et al.* 2006).
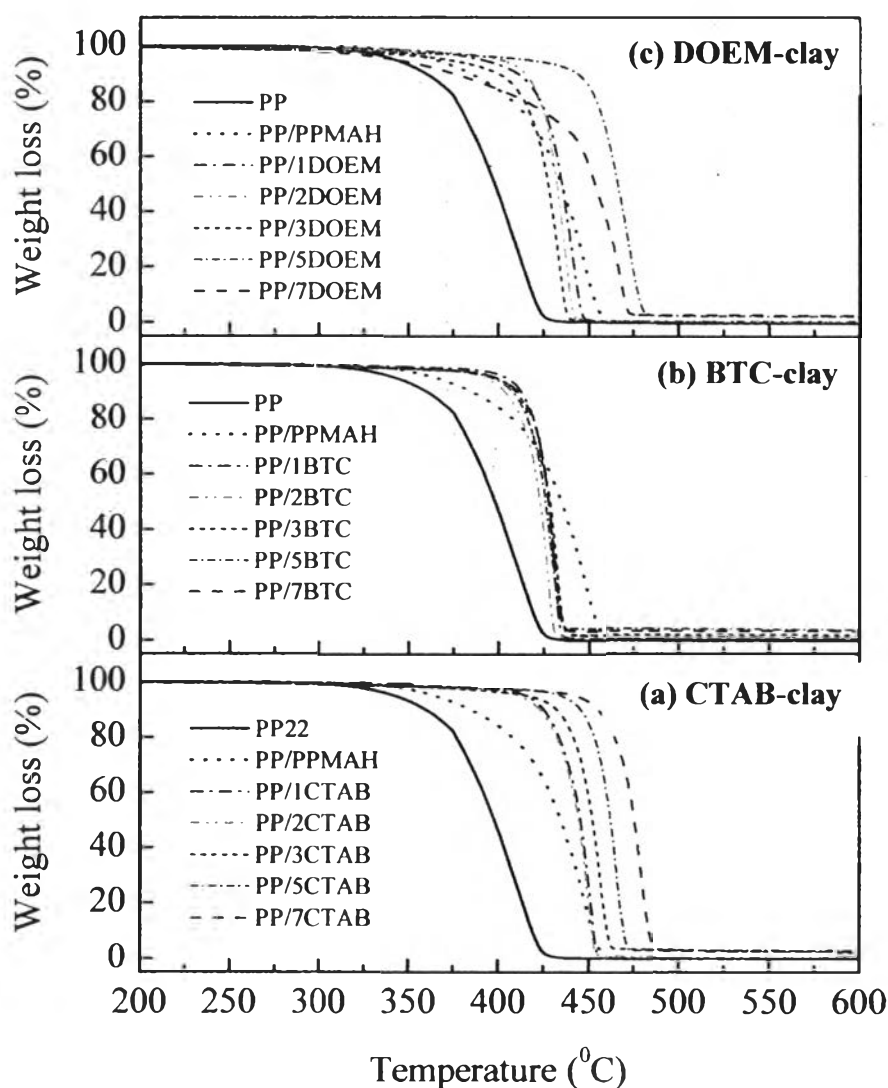
Figure 4.5 TGA thermograms of PP/organoclay nanocomposites for different types of organoclay (a) CTAB-clay, (b) BTC-clay, and (c) DOEM-clay.

4.3.5 Crystallization Behavior of PP/Organoclay Nanocomposites

Crystalline phase of PP/organoclay nanocomposites were investigated. The WAXD deconvolution results, carried out by a curve-fitting program given an example for PP, are in shown Figure 4.6. The same manner was applied for the rest. The WAXD patterns and %crystallinity of all nanocomposites are shown in Figure 4.7(a)-(c)) and Table 4.2, respectively. In general, isotactic polypropylene (iPP) can occur in three crystalline forms: α, β and γ phase. The monoclinic α-form is the most stable and is well documented (Padden, 1959; Natta, 1960; Turner-Jones, 1964). The β-form is formed only at specific conditions, being thermodynamically less stable than the α-form, but having a higher growth rate (Padden et al. 1959). While the γ-phases is preferentially formed under pressure (Meille et al. 1990). It is clear from WAXD patterns that the crystal phase of PP, PP/PPMAH and all nanocomposiytes is α-form, showing the reflections at 14°, 17°, 18.5°, 21°, 22°, 25.5°, and 28.5°, which assigned to planes of the monoclinic crystals (110), (040), (130), (111), (131)+(041), (060), and (220), respectively. This result indicates that the addition of the organoclay did not affect the crystallographic of PP confirmed by no change in melting temperature (T_m), as already reported by Xu et al. (2003).

The DSC analysis was carried out in order to illustrate more clearly the effect of organoclay loading to the crystallization behavior of PP. The melting and crystallization temperatures (T_m and T_c, respectively), as well as the melting enthalpy (ΔH_m) and degree of crystallinity (χ_c), calculated from the second heating run, are summarized in Table 4.2. As common expectation, the nanodispersed of layered silicate particle can act as an efficient heterogeneous nucleating agent and facilitate the crystallization of the nanocomposites, resulting in a higher crystallization temperature (He, 2003 and Wang, 2004). However, the crystallization behavior of nanocomposite will not be monotonically improved through the addition of a large amount of organoclay if the filler network plays a role to restrict the movement of molecular chains (Wang et al. 2006). Evidently, from Table 4.2, the crystallization temperature for most nanocomposites first increases with the addition of the organoclays, but then decreases or remains constant as the organoclay content exceeds 1wt%, although in this case the crystallization temperatures of

nanocomposites were higher than that of neat PP. Similarly, the crystallinity (χ_c) obtained from WAXD deconvolution, exhibited an increase at low amount of organoclay, followed by a decrease at higher amount of the organoclay. Comparing three types of nanocomposites, DOEM-clay based nanocomposites played role for the improvement in crystallization process of PP particularly at low volume fraction of the organoclay.
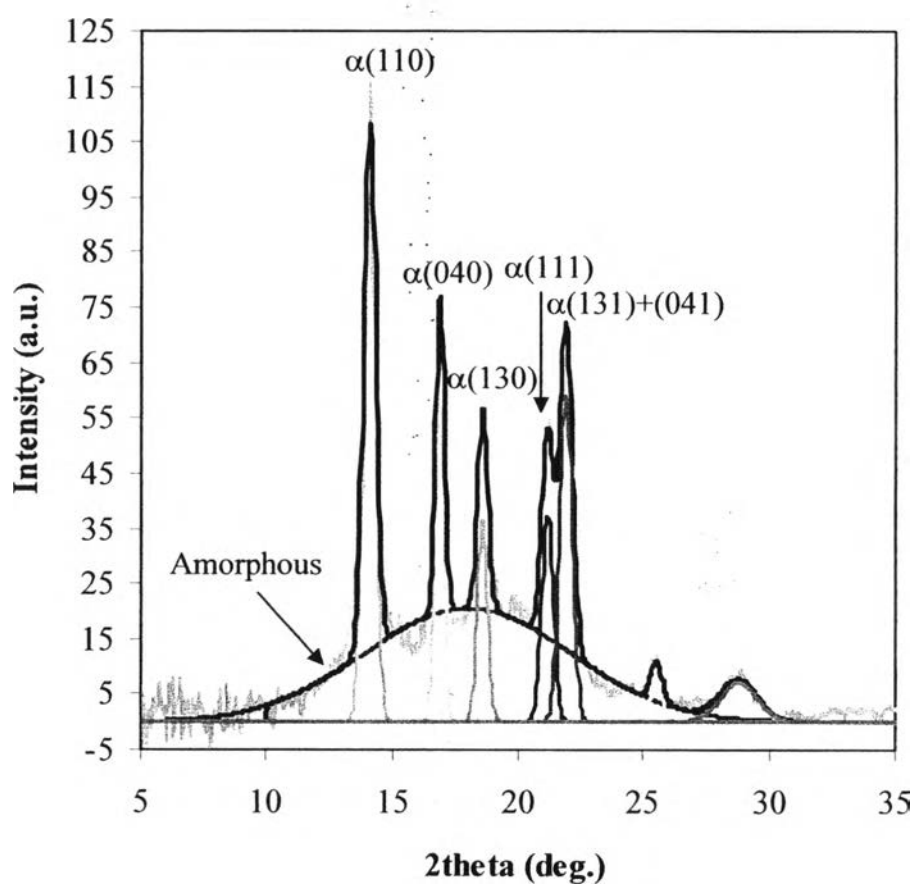
Figure 4.6 Typical peak deconvolution of amorphous and crystalline components of the PP WAXD profile.
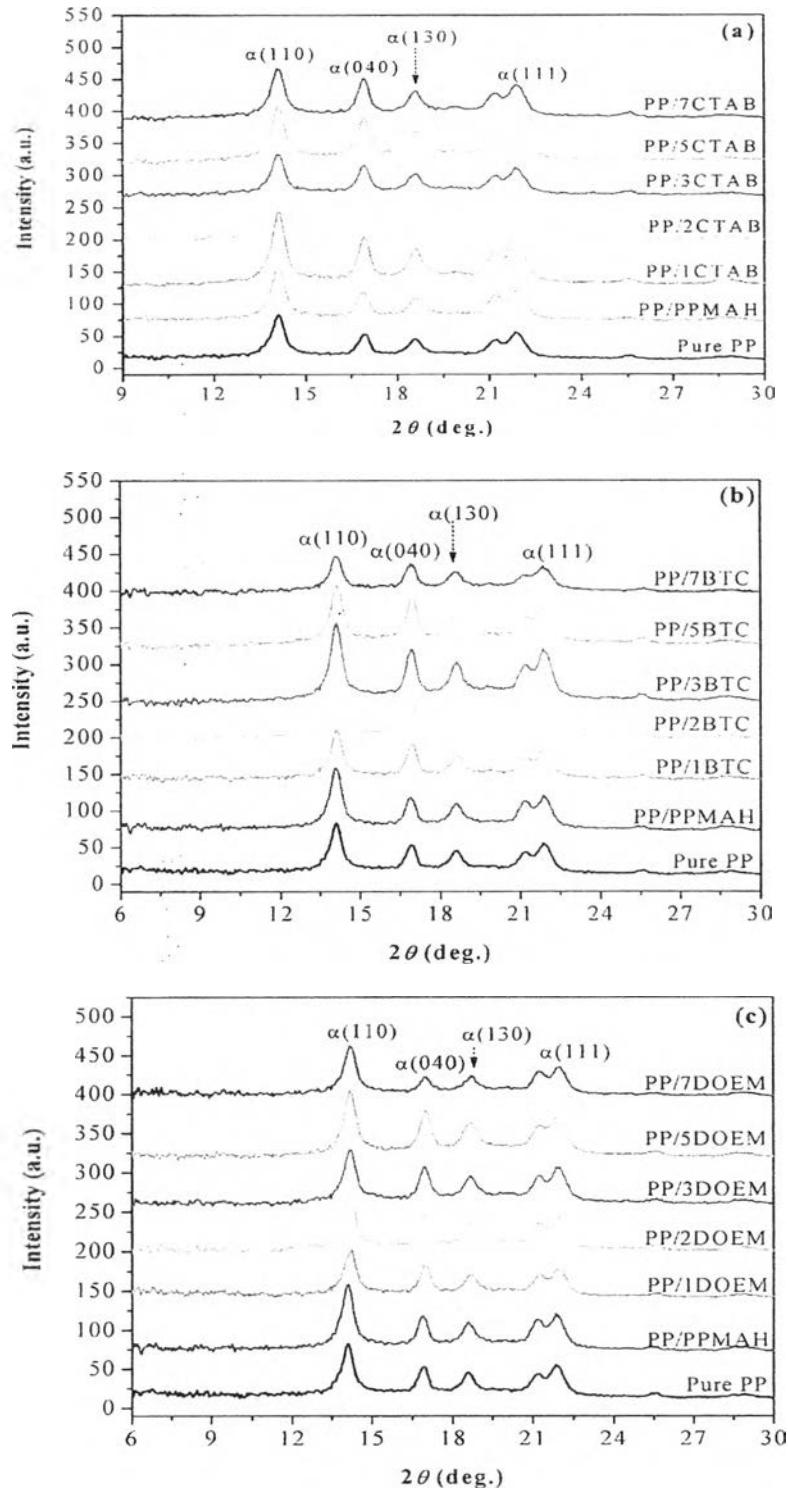
Figure 4.7 WAXD patterns for different types of PP/orgnoclay nanocomposites: (a) CTAB-clay, (b) BTC-clay, and (c) DOEM-clay.

Table 4.3 The degradation temperature at 10 and 50% weight loss ($T_{10\%}$ and $T_{50\%}$), melting (T_m) and crystallization temperature (T_c) and crystallinity (χ_c) of various PP/organoclay nanocomposites

PP/PPMAH/Organoclay	$T_{10\%}$ (°C)	$T_{50\%}$ (°C)	T_c (°C)	T_m (°C)	ΔH_m (J/g)	χ_c^a (%)	χ_c^b (%)
Pure PP (100)	358.9	398.1	120.6	160.4	71.1	34.3	46.1
PP/PPMAH (85/15/0)	384.0	434.6	123.9	161.1	80.5	38.9	47.0
PP/1CTAB (84/15/1)	424.8	456.8	123.4	161.0	79.7	38.9	48.2
PP/2CTAB (83/15/2)	448.1	468.1	121.5	160.4	76.9	37.9	46.9
PP/3CTAB (82/15/3)	454.4	473.8	121.5	160.3	76.1	37.9	44.4
PP/5CTAB (80/15/5)	431.9	452.0	121.4	160.6	77.7	39.5	47.4
PP/7CTAB (78/15/7)	452.1	468.4	121.4	160.6	77.3	40.1	44.7
PP/1BTC (84/15/1)	412.4	427.5	122.1	160.2	75.7	36.9	44.7
PP/2BTC (83/15/2)	403.2	422.9	121.0	160.6	83.9	41.3	44.6
PP/3BTC (82/15/3)	409.4	428.3	121.3	160.3	76.7	38.2	47.5
PP/5BTC (80/15/5)	407.4	425.7	120.9	160.3	74.5	37.9	46.5
PP/7BTC (78/15/7)	410.1	427.5	120.8	160.2	71.8	37.3	40.4
PP/1DOEM (84/15/1)	410.4	435.1	123.9	160.9	71.3	34.8	5.00
PP/2DOEM(83/15/2)	414.8	432.5	123.4	160.8	68.4	33.7	51.3
PP/3DOEM(82/15/3)	399.5	427.5	123.8	161.1	78.1	38.9	46.3
PP/5DOEM(80/15/5)	443.0	466.1	123.9	161.4	79.4	40.4	47.2
PP/7DOEM(78/15/7)	374.2	453.2	123.6	161.7	79.5	41.3	43.8

[a]Calculated as follows: $\chi_c=[\Delta H_m/(f^* \Delta H_m^0)]^*100$, where ΔH_m is the experimental melting enthalpy, f is the polypropylene fraction by weight in the composite and ΔH_m^0 is the melting enthalpy of infinite polypropylene crystal (207.1 J/g).

[b]Estimated from WAXD profile after a linear background subtraction and deconvolution of the profile into crystalline and amorphous fractions, using Gaussian lineshape for the peaks.
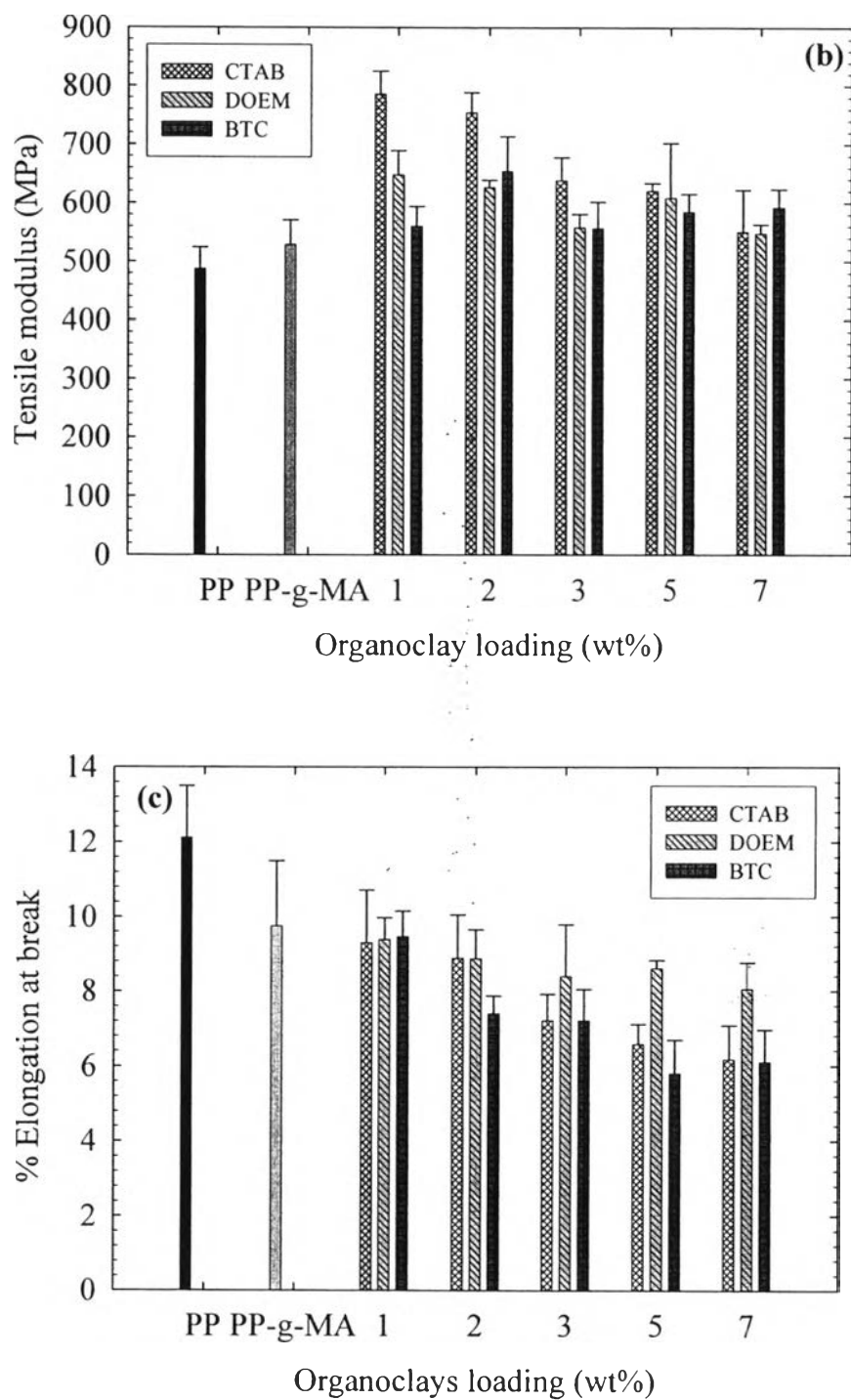
4.3.6 Mechanical Properties of PP/Organoclay Nanocomposites

The structure of the organic modifier used to form the organoclay is expected to have some effect on the morphology as well as mechanical properties of the nanocomposites. Well-dispersed nanofillers, of course, can improve the modulus and strength and maintain or even improve ductility because their small size does create large stress concentrations. In addition, the large interfacial area of nanocomposites provides an opportunity for altering the matrix properties in unique ways. Figure 4.8(a)-(c) show tensile modulus, tensile strength and elongation at break, respectively of nanocomposites as a function of organoclay type and loading. For the CTAB-clay and BTC-clay PP nanocomposites, there was a sharp increase in tensile strength and modulus when small amount of organoclay was added (i.e. 1 and 2 wt%). With an increase organoclay loading up to 7 wt%, tensile strength slightly decreases as compared to the pure PP and PP/PPMAH. For DOEM-clay based nanacomposites, at 1-5 wt% organoclay, there seems no significant effect on both tensile and modulus. When organoclay loading exceed 5 wt%, in contrast, tensile strength decreases markedly. A similar trend was observed for tensile modulus (Figure 4.8(b)). The increase in tensile strength at lower amount of organoclay loading might be attributed to the good interactions between the polymer and the organoclay filler, and thus the stress is much more efficiently transferred from polymer matrix to the inorganic filler, resulting in a greater improvement in tensile properties (Manias 2001 and Svoboda 2002). However, at higher organoclay loading, tensile strength and modulus decrease due to the aggregation of the silicate layers, tactiods or even the percolated network structures which act as the stress concentrators that allowing crack initiation and propagation, consequently decreasing the mechanical performance of the nanocomposites (Wang *et al.* 2006)

In contrast to the tensile strength and modulus, the elongation at break of nanocomposites reduces drastically with increasing the organoclay content as shown in Figure 4.8(c). The reduction of elongation might be due to the greater interaction between the filler and the polymer matrix, which probably affects to the lower chain mobility and then making the material more rigid (Modesti *et al.* 2005). Interestingly, for PP/DOEM-clay nanocomposites show a high value of elongation at break, particularly at higher amount of organoclay as compared to the others.

The improvement in elasticity may be due attributed in part to the plasticizing effect of the gallery DOEM surfactants having two long alkyl chains (2C18) and to their contribution to the formation of dangling chains but also probably to conformational effects at the clay–matrix interface (Wang and Pinnavia, 1998). Among three types of nanocomposites, BTC-clay nanocomposite shows the lowest value. In other word, the nanocomposite based on one chain or two long chains modified clay play role in mechanical properties improvement rather than voluminous organoclay based nanocomposites.
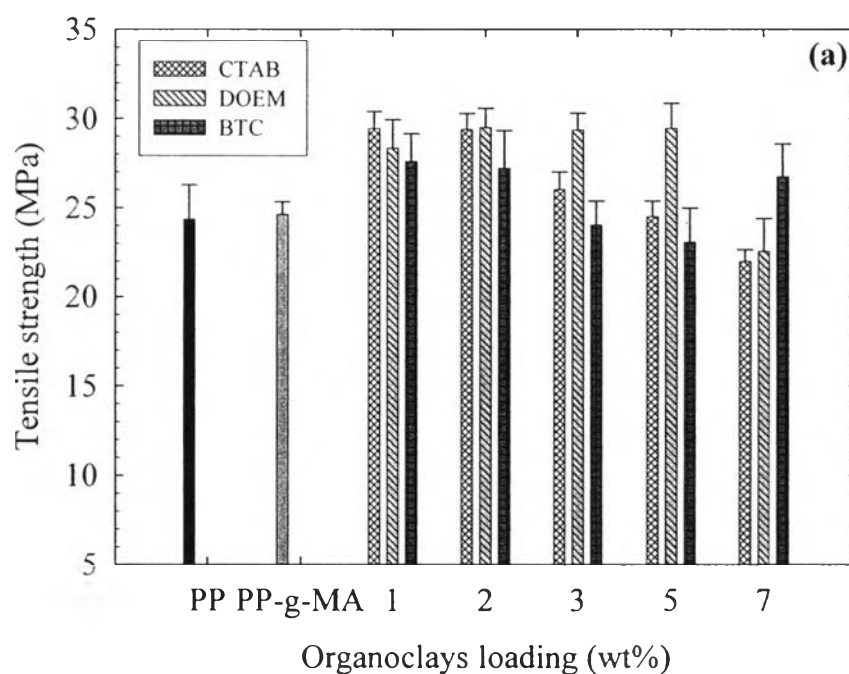
Figure 4.8 Mechanical properties of different PP/organoclay nanocomposites: (a) Tensile strength, (b) Tensile modulus, and (c) %Elongation at break.

4.4 Conclusions

Polypropylene (PP)/organoclay nanocomposites with three different types of alkyl ammonium surfactants were successfully prepared by melt intercalation technique in a co-rotating twin screw extruder. The polypropylene-graft-maleic anhydride (PP-g-MA) was used as a compatibilizer and the amount of each organoclay was varied from 1 to 7 wt%. The effect of alkyl ammonium surfactant structures and amount of organoclay were investigated. From the XRD result, the nanocomposites prepared from CTAB-clay and BTC-clay showed the intercalated morphology, while the nanocomposite prepared from DOEM-clay showed the partially exfoliated structure. All nanocomposites showed improvement in both thermal and mechanical properties as compared to the pure PP and PP/PP-g-MA system. Among three types of alkyl ammonium surfactants, the nanocomposite prepared from DOEM, having two tails and the longest alkyl chain length (C18), gave the best properties in term of morphology and physical property due to the better clay dispersion. While the nanocomposites prepared from CTAB-clay revealed the highest thermal stability.